Development 138, 3509-3518 (2011) doi:10.1242/dev.069740
© 2011. Published by The Company of Biologists Ltd

Microtubule-based localization of a synaptic calcium-signaling complex is required for left-right neuronal asymmetry in *C. elegans*

Chieh Chang[1], Yi-Wen Hsieh[1], Bluma J. Lesch[2], Cornelia I. Bargmann[2] and Chiou-Fen Chuang[1,*]

SUMMARY

The axons of *C. elegans* left and right AWC olfactory neurons communicate at synapses through a calcium-signaling complex to regulate stochastic asymmetric cell identities called AWC^{ON} and AWC^{OFF}. However, it is not known how the calcium-signaling complex, which consists of UNC-43/CaMKII, TIR-1/SARM adaptor protein and NSY-1/ASK1 MAPKKK, is localized to postsynaptic sites in the AWC axons for this lateral interaction. Here, we show that microtubule-based localization of the TIR-1 signaling complex to the synapses regulates AWC asymmetry. Similar to *unc-43*, *tir-1* and *nsy-1* loss-of-function mutants, specific disruption of microtubules in AWC by nocodazole generates two AWC^{ON} neurons. Reduced localization of UNC-43, TIR-1 and NSY-1 proteins in the AWC axons strongly correlates with the 2AWC^{ON} phenotype in nocodazole-treated animals. We identified kinesin motor *unc-104/kif1a* mutants for enhancement of the 2AWC^{ON} phenotype of a hypomorphic *tir-1* mutant. Mutations in *unc-104,* like microtubule depolymerization, lead to a reduced level of UNC-43, TIR-1 and NSY-1 proteins in the AWC axons. In addition, dynamic transport of TIR-1 in the AWC axons is dependent on *unc-104*, the primary motor required for the transport of presynaptic vesicles. Furthermore, *unc-104* acts non-cell autonomously in the AWC^{ON} neuron to regulate the AWC^{OFF} identity. Together, these results suggest a model in which UNC-104 may transport some unknown presynaptic factor(s) in the future AWC^{ON} cell that non-cell autonomously control the trafficking of the TIR-1 signaling complex to postsynaptic regions of the AWC axons to regulate the AWC^{OFF} identity.

KEY WORDS: *C. elegans*, Microtubules, Olfactory development, Left-right asymmetry, Calcium signaling

INTRODUCTION

The left and right sides of the central nervous system display anatomical, molecular and functional asymmetries throughout the animal kingdom. Functional lateralization in the brain is theorized to increase cognitive performance and social behaviors, as reduced and reverse anatomical brain asymmetry has been linked to a variety of neurodevelopmental disorders (Taylor et al., 2010). However, the mechanisms underlying lateralization of the developing nervous system remain poorly understood.

Like the vertebrate central nervous system, the *C. elegans* nervous system displays molecular and functional asymmetries (Hobert, 2006; Hobert et al., 2002; Sagasti et al., 2001; Taylor et al., 2010). In both ASE taste neurons and AWC olfactory neurons, the left and right neurons of a pair have different patterns of gene expression and respond to different sets of chemicals (Pierce-Shimomura et al., 2001; Troemel et al., 1999; Wes and Bargmann, 2001; Yu et al., 1997). However, the mechanisms that specify ASE and AWC asymmetries are completely distinct. The ASE neurons develop a stereotyped asymmetry early in embryogenesis, whereas the AWC neurons develop stochastic asymmetry late in embryogenesis (Chuang and Bargmann, 2005; Poole and Hobert, 2006). None of the identified ASE asymmetry genes affects AWC asymmetry and, conversely, AWC asymmetry genes do not affect ASE asymmetry (Chang et al., 2003; Koga and Ohshima, 2004; Lanjuin et al., 2003; Lesch et al., 2009).

In wild-type animals, the reporter gene *str-2p::GFP* is expressed in only one of the two AWC neurons, and never in both (Fig. 1A). The two AWC neurons are described as AWC^{ON}, which expresses *str-2p::GFP*, and AWC^{OFF}, which does not. The expression of *str-2p::GFP* in AWC is random: 50% of the animals in a population express *str-2* in the left AWC neuron, whereas the other 50% express *str-2* in the right AWC. Genetic studies and cell killing experiments suggest that AWC^{OFF} is the default state and asymmetric expression of *str-2* requires an interaction between the two AWC neurons (Troemel et al., 1999).

Genetic screens identified several genes that regulate AWC asymmetry. Loss-of-function or reduction-of-function mutations in a calcium-regulated signaling pathway, including a voltage-gated calcium channel (UNC-2, EGL-19, UNC-36), the calcium/calmodulin-dependent protein kinase II (CaMKII) UNC-43, the Toll-interleukin 1 repeat protein TIR-1/SARM, the mitogen-activated protein kinase kinase kinase (MAPKKK) NSY-1/ASK1 and the MAPKK SEK-1 kinase cascade, lead to animals with two AWC^{ON} (Fig. 1C; 2AWC^{ON} phenotype) and no AWC^{OFF} cells. These results suggest that these genes normally promote the default AWC^{OFF} identity (Bauer Huang et al., 2007; Chuang and Bargmann, 2005; Sagasti et al., 2001; Tanaka-Hino et al., 2002; Troemel et al., 1999). An innexin gap junction protein, encoded by *nsy-5*, and a claudin-like protein, encoded by *nsy-4*, function in parallel to inhibit the downstream calcium-regulated signaling pathway in the neuron that acquires the AWC^{ON} identity (Chuang et al., 2007; VanHoven et al., 2006). When the activity of *nsy-4* or *nsy-5* is reduced or lost, mutant animals fail to induce the AWC^{ON} cell, leading to the formation of

[1]Division of Developmental Biology, Children's Hospital Medical Center Research Foundation, 240 Albert Sabin Way, Cincinnati, OH 45229, USA. [2]Howard Hughes Medical Institute, Laboratory of Neural Circuits and Behavior, The Rockefeller University, New York, NY 10065, USA.

*Author for correspondence (chiou-fen.chuang@cchmc.org)

Accepted 10 June 2011

two AWC^{OFF} cells (2AWC^{OFF} phenotype). NSY-5 forms transient gap junctions between the cell bodies of the AWCs and their neighboring neurons in embryos. Genetic analysis suggests that communication between the two AWCs and other neurons in the NSY-5 gap junction network is required for the induction of AWC asymmetry (Chuang et al., 2007). Once AWC asymmetry is specified in late embryogenesis, both the AWC^{ON} and AWC^{OFF} identities are maintained throughout the life of the worm by cGMP signaling, dauer pheromone signaling and transcriptional repressors. Animals with mutations in maintenance pathways have wild-type AWC asymmetry in the first larval stage, but display mutant AWC phenotypes in the adult stage (Lesch and Bargmann, 2010; Lesch et al., 2009; Troemel et al., 1999).

TIR-1/SARM functions as an adaptor protein to couple upstream UNC-43/CaMKII and downstream NSY-1/ASK1 MAPKKK signaling at postsynaptic regions in the AWC axons for the regulation of AWC^{OFF} identity (Chuang and Bargmann, 2005). Proper localization of these calcium signaling proteins at AWC synapses is important for the regulation of AWC asymmetry, but it is not understood how the AWC asymmetry signaling complex is targeted to the synapses. Here, we show that microtubules and microtubule-dependent kinesin motor UNC-104/KIF1A control the synaptic localization of the TIR-1 signaling complex to regulate left-right AWC asymmetry.

MATERIALS AND METHODS

Strains

Wild-type strains were *C. elegans* variety Bristol, strain N2. Strains were maintained by standard methods (Brenner, 1974). Mutations and integrated transgenes used in this study included: *kyIs140 [str-2p::GFP; lin-15(+)] I* (Troemel et al., 1999), *vyIs2 [odr-3p::tir-1::GFP; ofm-1p::DsRed] I*, *nsy-5(ky634) I* (Chuang et al., 2007), *unc-104(rh142) II*, *unc-104(rh43) II*, *unc-104(e1265) II*, *kyIs323 [str-2p::GFP; ofm-1p::GFP]* II, *ben-1(e1880)* III, *tir-1(tm3036) III*, *tir-1(ky388ts) III* (Chuang and Bargmann, 2005), *tir-1(ky648gf) III*, *unc-43(n498gf)IV*, *oyIs44 [odr-1p::DsRed] V*, *vyIs51 [str-2p::2xnlsTagRFP; ofm-1p::DsRed] V*, and *vyIs48 [odr-3p::tir-1::DsRed; odr-3p::unc-43::GFP; str-2p::nlsCFP; ofm-1p::DsRed]*.

Transgenes maintained as extrachromosomal arrays included: *vyEx1123, 1124 [odr-3p::ben-1::SL2::TagRFP; ofm-1p::DsRed]*, *vyEx668, 677, 678 [odr-3p::tir-1^{A538V}::GFP; str-2p::nlsCFP; ofm-1p::DsRed]*, *vyEx669, 670, 673 [odr-3p::tir-1::GFP; str-2p::nlsCFP; ofm-1p::DsRed]*, *kyEx588 [odr-3p::nsy-1(gf); myo-3p::DsRed]* (Chuang and Bargmann, 2005), *vyEX1103, 1104 [odr-3p::nsy-1::GFP; ofm-1p::DsRed]*, *vyEx1020, 1029, 1037 [odr-3p::unc-104; odr-1p::DsRed; ofm-1p::DsRed]*, *vyEx944, 945, 946 [unc-104p::unc-104; odr-1p::DsRed; ofm-1p::DsRed]*, *vyEx925 [unc-104p::GFP; ofm-1p::DsRed]*, *vyEx779, 780, 787 [odr-3p::tir-1::DsRed; odr-3p::unc-104::GFP; ofm-1p::DsRed]*, *vyEx611, 615 [odr-3p::GFP; elt-1p::CFP]*; and *vyEx1101, 1102 [odr-3p::unc-43::GFP; ofm-1p::DsRed]*.

Plasmid construction and germline transformation

A 4.2 kb PCR fragment of *unc-104* promoter was subcloned into pPD95.77 to make *unc-104p::GFP*. *ben-1* cDNA (1332 bp) and *unc-104* cDNA (4752 bp) were obtained with RT-PCR of total mRNA from mixed stage worms and subcloned to make *odr-3p::ben-1::SL2::TagRFP*, *odr-3p::unc-104*, *unc-104p::unc-104* and *odr-3p::unc-104::GFP*. *odr-3p::tir-1^{A538V}::GFP* was generated by site-directed mutagenesis (Stratagene QuikChange kit). *str-2p::nlsCFP* was made by replacing the *myo-3* promoter in *myo-3p::nlsCFP* (pPD133.45) with 3.7 kb of the *str-2* promoter (Troemel et al., 1999). *str-2p::2xnlsTagRFP* was made by cloning the *str-2* promoter in a 2xnlsTagRFP vector (a gift from Oliver Hobert, Columbia University Medical Center, NY, USA).

odr-3p::ben-1::SL2::TagRFP (50 ng/μl), *odr-3p::tir-1::GFP* (5 ng/μl), *odr-3p::tir-1^{A538V}::GFP* (5 ng/μl), *odr-3p::tir-1::DsRed* (10 ng/μl), *odr-3p::unc-43::GFP* (8 ng/μl), *odr-3p::nsy-1::GFP* (10 ng/μl), *odr-3p::GFP* (10 ng/μl), *odr-3p::unc-104* (50 ng/μl), *unc-104p::unc-104* (30 ng/μl), *odr-3p::unc-104::GFP* (6 ng/μl), *unc-104p::GFP* (25 ng/μl), *odr-1p::DsRed* (15 ng/μl), *str-2p::nlsCFP* (100 ng/μl), *str-2p::2xnlsTagRFP* (50 ng/μl), *ofm-1p::DsRed* (30 ng/μl), and *elt-2p::CFP* (7.5 ng/μl) were injected into animals as described previously (Mello and Fire, 1995).

Nocodazole and benomyl treatment of worm embryos

To stage embryos, adults were allowed to lay eggs for 2 hours, then adults were removed from the plates. Laid embryos were cultured on plates for varying time until they were treated with drugs (see Fig. S1 in the supplementary material). Gravid adults were bleached with 20% clorox to collect early stage embryos. Collected embryos were bleached to increase the permeability of the eggshell to drugs and then treated with 150 μM nocodazole (Sigma M1404, dissolved in DMSO) or benomyl (Sigma 45339, dissolved in DMSO) or DMSO (as a control) for 2 hours. DMSO treatment did not affect AWC asymmetry or the localization of UNC-43/TIR-1/NSY-1 in the AWC axons.

Genetic mosaic analysis

Mosaic analysis and statistical analysis were performed as previously described (Bauer Huang et al., 2007; Sagasti et al., 2001; VanHoven et al., 2006). Expected numbers of mosaic animals were predicted from internal control animals, which retained the *unc-104p::unc-104; odr-1p::DsRed* transgene in both AWC neurons, from the same transgenic line. Expected and observed numbers of mosaic animals were compared using the chi-square test with three degrees of freedom.

Dynamic imaging

Dynamic imaging was performed on an inverted Nikon TE2000U microscope equipped with a Hamamatsu ORCA-AG high speed CCD digital camera and a Nikon 100× 1.4 objective. Worms in the L1 larval stage were mounted onto 2% agarose pads and anesthetized with 6 mM levamisole (Sigma) for imaging. Movies were acquired for 20-40 seconds with a speed of seven frames per second and an exposure time of 140 mseconds. Movies were analyzed using the ImageJ software.

RESULTS

Microtubules are required for left-right AWC neuronal asymmetry

Microtubules have been implicated in left-right patterning in several organisms (Abe et al., 2004; Levin and Palmer, 2007; Nonaka et al., 1998; Supp et al., 1997; Takeda et al., 1999; Thitamadee et al., 2002). Microtubules are polymers of tubulin heterodimers, which contain different α- and β-tubulin isotypes encoded by separate genes. There are nine α-tubulin and six β-tubulin isoforms predicted in the *C. elegans* genome (*C. elegans* Sequencing Consortium, 1998). Previous studies suggested functional redundancy of some α- and β-tubulin isotypes (Driscoll et al., 1989; Lu et al., 2004; Phillips et al., 2004; Wright and Hunter, 2003). Nocodazole, which disrupts microtubule polymerization regardless of subunit composition, provides a convenient tool with which to analyze the function of microtubules in biological processes. To test for a potential role of microtubules in the establishment of AWC asymmetry, wild-type animals containing the *str-2p::GFP* transgene were treated with nocodazole for 2 hours at different embryonic stages and in the first larval (L1) stage, and adults were scored for *str-2p::GFP* expression in AWC.

The AWC neurons are born at about 1 hour after egg laying and their axons extend at about 3.5 hours after egg laying. *tir-1* function must be present by late embryogenesis (~8 hours after egg laying) to generate AWC asymmetry, suggesting that the crucial period for the establishment of AWC asymmetry is before the late embryo stage (Chuang and Bargmann, 2005). Nocodazole treatment of embryos before egg laying or at 0-6 hours after egg laying led to the expression of *str-2p::GFP* in both AWC neurons, a 2AWC^{ON} phenotype (Fig. 1B; see Fig. S1 in the supplementary material). Nocodazole-treated animals with two AWC^{ON} neurons also

DEVELOPMENT

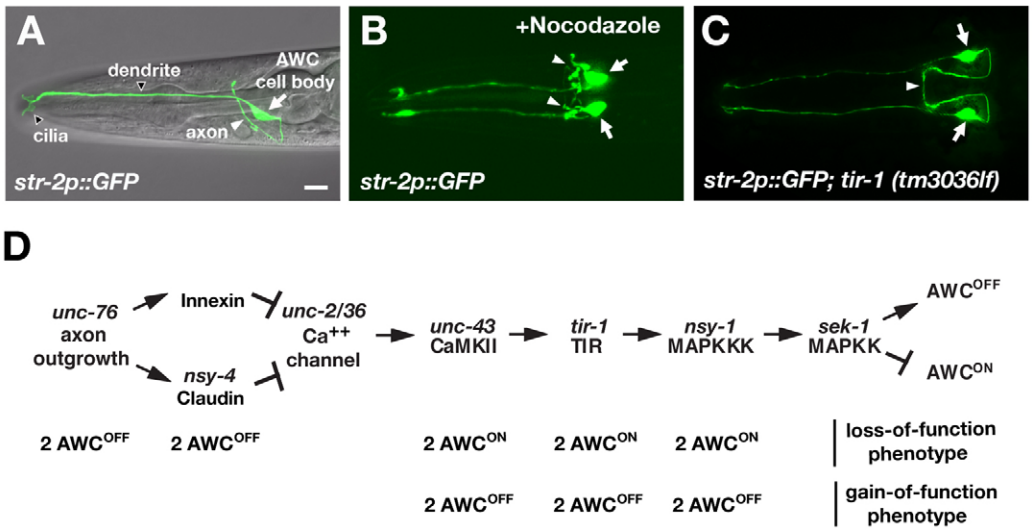

Fig. 1. Nocodazole treatment disrupts left-right AWC asymmetry. (**A-C**) Expression of the reporter gene *str-2p::GFP* in wild-type (A), nocodazole-treated (B) and *tir-1(tm3036lf)* (C) animals. In some of nocodazole-treated animals, the AWC axons are distorted, as indicated by arrowheads (B). Scale bar: 10 μm. Anterior is leftwards and ventral is towards the bottom. Arrows indicate the AWC cell bodies. (**D**) The AWC signaling pathway.

displayed slow growth, dumpy morphology, and/or uncoordinated locomotion phenotypes. However, nocodazole treatment of embryos at 6-8 hours after egg laying or during the first larval stage (~13 hours after egg laying) did not cause a 2AWC^{ON} phenotype (see Fig. S1 in the supplementary material). These results suggest that nocodazole needs to be present before and/or during the crucial period for *tir-1* function to affect AWC asymmetry. In subsequent studies, mixed stages of embryos before and after egg laying were used for nocodazole or benomyl (another inhibitor of microtubule polymerization) treatment and only slower-growing adults were scored for AWC phenotypes. We also observed a 2AWC^{ON} phenotype at a lower frequency than nocodazole treatment when embryos were treated with benomyl (Table 1, rows b and c). Benomyl-treated animals sometimes displayed a weak 2AWC^{OFF} phenotype. Some of the 2AWC^{ON} animals resulting from benomyl or nocodazole treatment had truncated and disoriented AWC axons (Fig. 1B). Mutants such as *unc-76* loss-of-function alleles disrupt axon outgrowth of AWC neurons, but generate a 2AWC^{OFF} phenotype (Troemel et al., 1999), the opposite phenotype from the 2AWC^{ON} phenotype of nocodazole- or benomyl-treated animals. These results suggest that nocodazole and benomyl must affect a different aspect of AWC development in addition to any possible effects on axon outgrowth.

Loss-of-function mutations in *ben-1*, which encodes a β-tubulin, confer resistance to benzimidazoles such as nocodazole and benomyl (Driscoll et al., 1989). To determine whether the 2AWC^{ON} phenotype is due to disruption of microtubules, we examined the effect of nocodazole on *ben-1* mutants. *ben-1(e1880)* mutants showed wild-type expression of *str-2*, and treatment of *ben-1(e1880)* mutant embryos with nocodazole did not cause a 2AWC^{ON} phenotype (Table 1, rows d and e). However, expression of wild-type *ben-1* gene primarily in AWC using an *odr-3* promoter (Roayaie et al., 1998) restored the susceptibility of *ben-1(e1880)* mutants to nocodazole in the generation of 2AWC^{ON} phenotype (Table 1, rows f and g). These results suggest that the 2AWC^{ON} phenotype in nocodazole-treated animals is caused by specific disruption of microtubules in AWC.

Nocodazole treatment may affect the function of the TIR-1 signaling complex in AWC asymmetry

The molecular signaling pathway that regulates AWC asymmetry involves a calcium-regulated kinase pathway including *unc-43* (CaMKII), *tir-1* (SARM/adaptor protein) and *nsy-1* (ASK1/MAPKKK) (Chuang and Bargmann, 2005; Sagasti et al., 2001; Troemel et al., 1999) (Fig. 1D). Loss-of-function mutants of *unc-43*, *tir-1* or *nsy-1* showed a 2AWC^{ON} phenotype resembling that caused by nocodazole treatment (Fig. 1B,C). This similarity suggests that the nocadazole-induced 2AWC^{ON} phenotype could result from defects in the calcium-regulated CaMKII-TIR-1-NSY-1 signaling pathway.

To determine the potential role of nocodazole in the AWC signaling pathway, we treated different mutants affecting AWC asymmetry with nocodazole. As nocodazole treatment generated two AWC^{ON} cells, it was administered to the mutants with the opposite phenotype (two AWC^{OFF} cells) to determine the relationship of the nocodazole target with other genes in the AWC pathway. The interaction between nocodazole and mutations was analyzed using the same principles as genetic analysis of double mutants. Loss-of-function (lf) mutations in the *nsy-5* innexin genes or gain-of-function (gf) mutations in *unc-43*, *tir-1* and *nsy-1*, which cause two AWC^{OFF} cells, (Chuang et al., 2007; Chuang and Bargmann, 2005; Sagasti et al., 2001; Troemel et al., 1999) (Fig. 1D) were treated with nocodazole. Nocodazole treatment of *nsy-5(lf)* or *unc-43(gf)* mutants strongly suppressed their 2AWC^{OFF} phenotype and generated a 2AWC^{ON} phenotype (Table 1, rows h, i, k, l). These results are consistent with the effect of nocodazole on signaling predominantly downstream of or parallel to *nsy-5* and *unc-43*. By contrast, the 2AWC^{ON} phenotype resulting from nocodazole treatment was greatly suppressed by *nsy-1(gf)* mutants (Table 1, rows t, u). This result suggests that nocodazole acts on a target mainly upstream of or parallel to *nsy-1*.

These results are consistent with a model in which nocodazole affects the AWC signaling step downstream of/parallel to *unc-43* CaMKII and upstream of/parallel to *nsy-1* MAPKKK. Previous genetic studies suggest that *tir-1* also acts downstream of *unc-43*

DEVELOPMENT

Table 1. Effect of nocodazole and benomyl treatment on *str-2* expression in AWC

Genetic background	Row	Treatment	$2AWC^{OFF}$ (%)	$1AWC^{OFF}/1AWC^{ON}$ (%)	$2AWC^{ON}$ (%)	*n*
Wild type	a	–	1	99	0	188
	b	Benomyl	6	84	10	127
	c	Nocodazole	0	64	36	220
ben-1(e1880)	d	–	0	100	0	163
	e	Nocodazole	3	97	0	165
ben-1(e1880); odr-3p::ben-1	f	–	14	86	0****	129
	g	Nocodazole	7	62	31****	122
nsy-5(ky634lf)	h	–	98****	2	0	218
	i	Nocodazole	45****	33	22	51
unc-43(n498gf), L1	j	–	80	20**	0	70
unc-43(n498gf)	k	–	95****	5**	0	112
	l	Nocodazole	21****	51	28	108
tir-1(ky648gf), L1	m	–	63	37****	0	112
tir-1(ky648gf)	n	–	91****	9****	0	151
	o	Nocodazole	29****	60	11	108
tir-1(tm3036lf)	p	–	0	0	100	111
tir-1(tm3036lf); odr-3p::tir-1^{A538V}::GFP	q	–	99	1	0	138
tir-1(tm3036lf); odr-3p::tir-1::GFP	r	–	0	100	0	147
odr-3p::nsy-1(gf), L1	s	–	44	56****	0	64
odr-3p::nsy-1(gf)	t	–	97 (ns)	3****	0	139
	u	Nocodazole	92 (ns)	7	1	85

Animals were scored as adults, unless otherwise indicated.
–, no treatment; ***P*=0.003; ****$P<0.0001$; ns, not significant. *Z*-test for two proportions.

CaMKII and upstream of *nsy-1* MAPKKK to regulate AWC asymmetry (Fig. 1D). Thus, we examined the interaction between *tir-1* and nocodazole. The *tir-1(ky648)* allele, in which a C to T mutation results in an alanine to valine substitution of the 538th amino acid of the TIR-1a isoform, was isolated from a genetic screen for mutants with a $2AWC^{OFF}$ phenotype (VanHoven et al., 2006). The strong $2AWC^{OFF}$ phenotype of *tir-1(ky648)* is the opposite of the *tir-1* loss-of-function $2AWC^{ON}$ phenotype (Table 1, rows n and p). We found that the transgene *odr-3p:: tir-1^{A538V}::GFP*, which expresses the mutant TIR-1^{A538V} protein tagged with GFP in AWC, suppressed the $2AWC^{ON}$ phenotype in *tir-1(tm3036lf)* mutants and also generated a strong gain-of-function $2AWC^{OFF}$ phenotype (Table 1, row q). By contrast, *odr-3p::tir-1::GFP*, when injected at the same low level as *odr-3p::tir-1^{A538V}::GFP*, rescued the *tir-1(tm3036lf)* mutant but did not cause a gain-of-function phenotype (Table 1, row r). These results suggest that *ky648* is a strong *tir-1* gain-of-function allele. Nocodazole treatment of *tir-1(ky648gf)* mutants significantly suppressed the $2AWC^{OFF}$ phenotype and also generated a $2AWC^{ON}$ phenotype (Table 1, row o). Together, these results are consistent with the hypothesis that nocodazole may modify the activity of the TIR-1 signaling complex.

Microtubules are required for the localization of TIR-1, UNC-43 and NSY-1 in the AWC axons to regulate the AWC^{OFF} identity

The axons of the two AWC neurons form chemical synapses on each other in the nerve ring, where axons from the left and right sides meet (White et al., 1986). Our previous results showed that TIR-1/SARM adaptor, UNC-43/CaMKII and NSY-1 ASK1/MAPKKK are enriched in postsynaptic regions of the AWC axons (Chuang and Bargmann, 2005). As the TIR-1 signaling complex is a possible target of nocodazole in the AWC signaling pathway, we investigated whether the subcellular localization of TIR-1, along with its signaling complex components UNC-43 and NSY-1, is regulated by microtubules.

unc-43, *tir-1* and *nsy-1* act to execute the AWC^{OFF} decision in late embryogenesis (Chuang and Bargmann, 2005; Sagasti et al., 2001). However, in *tir-1(ky648gf)* mutants, about 37% of animals had one AWC^{ON} neuron in the L1 stage (Table 1, row m), whereas the fraction of animals with one AWC^{ON} neuron significantly decreased to 9% in adults (Table 1, row n). These results suggest that *tir-1(ky648gf)* mutants are also defective in the maintenance of the AWC^{ON} identity. Similar to *tir-1(ky648gf)*, *unc-43(n498gf)* and *nsy-1(gf)* also displayed a defect in the maintenance of the AWC^{ON} state, with more animals exhibiting one AWC^{ON} neuron in the L1 stage than as adults (Table 1, rows j,k,s,t). These results reveal a role for *tir-1*, *unc-43 and nsy-1* in the suppression of the AWC^{ON} identity and/or promotion of the AWC^{OFF} identity in the L1 stage. Because late embryos constantly move and are poorly permeable to anesthetics such as sodium azide and levamisole, we chose to use the L1 stage for live imaging of fluorescently tagged proteins. In subsequent studies, we expressed TIR-1, UNC-43, NSY-1 and UNC-104 in AWC from the *odr-3* promoter and analyzed their localization patterns in the L1 stage. All of these transgenes encoded functional proteins and were injected at a low level that did not cause a gain-of-function phenotype in AWC asymmetry.

To test directly the effect of nocodazole on the localization of TIR-1, UNC-43, NSY-1 in the AWC axons and the function of these signaling proteins in AWC asymmetry, *odr-3p::tir-1::DsRed* was co-expressed with *str-2p::nls-CFP*, a nucleus-localized AWC^{ON} marker. Similarly, *odr-3p::unc-43::GFP* or *odr-3p::nsy-1::GFP* was co-expressed with *str-2p::nls-TagRFP*, a red nucleus-localized AWC^{ON} marker. These strains allowed simultaneous visualization of protein subcellular localization and AWC asymmetry in the same animal. The fluorescence intensity of TIR-1::DsRed, UNC-43::GFP and NSY-1::GFP in the AWC axons was examined and quantified in nocodazole-treated animals that exhibited $1AWC^{ON}/1AWC^{OFF}$ (hereafter, wild type) and $2AWC^{ON}$ phenotypes.

Although both wild-type and $2AWC^{ON}$ animals had TIR-1::DsRed puncta in their AWC axons, the numbers of puncta were significantly different ($P<0.0001$). Wild-type animals had an average of 5.4 TIR-1::DsRed puncta per animal (n=32), whereas $2AWC^{ON}$ animals had 1.6 puncta per animal (n=21) (data not shown). The average fluorescence intensity of TIR-1::DsRed in the AWC axons was also significantly reduced in $2AWC^{ON}$ animals

DEVELOPMENT

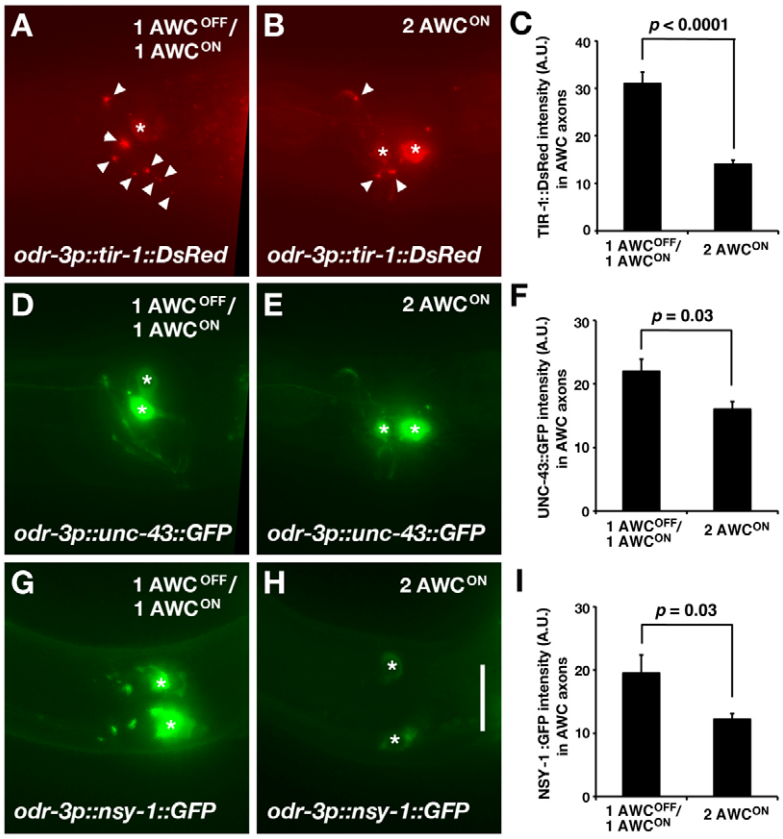

Fig. 2. Nocodazole disrupts synaptic localization of TIR-1, UNC-43 and NSY-1 in the AWC axons. (**A**,**B**) Images of TIR-1::DsRed in AWC neurons of nocodazole-treated animals exhibiting 1AWC^{OFF}/1AWC^{ON} (A) and 2AWC^{ON} (B) phenotypes. Arrowheads indicate TIR-1::DsRed puncta in the AWC axons. Asterisks indicate cell bodies. (**C**) The average intensity of TIR-1::DsRed in the AWC axons. (**D**,**E**) Images of UNC-43::GFP in AWC neurons of nocodazole-treated animals. (**F**) The average intensity of UNC-43::GFP in the AWC axons. (**G**,**H**) Images of NSY-1::GFP in AWC neurons of nocodazole-treated animals. (**I**) The average intensity of NSY-1::GFP in the AWC axons. Images were taken from L1 animals. Scale bar: 10 μm. A.U., arbitrary unit. Error bars indicate the s.e.m.; *t*-test; $n>15$ for each transgene in 1AWC^{OFF}/1AWC^{ON} or 2AWC^{ON} animals.

(Fig. 2A-C). In addition, expression of TIR-1::DsRed in the AWC cell body was stronger in 2AWC^{ON} animals than in wild type (Fig. 2A,B). These results reveal a tight link between microtubule-dependent TIR-1 localization in the AWC axons and AWC^{OFF} identity determination.

UNC-43::GFP and NSY-1::GFP were not as tightly localized in the AWC axons as TIR-1, thus we directly quantified their fluorescence intensity instead of measuring the puncta number. In wild type, both UNC-43::GFP and NSY-1::GFP were localized in a punctate pattern in the AWC axons with some diffuse expression in the AWC cell body (Fig. 2D,G). In 2AWC^{ON} animals, expression of both UNC-43::GFP and NSY-1::GFP was significantly reduced in the AWC axons (Fig. 2E,F,H,I). The expression level of UNC-43::GFP in the AWC cell body is similar in wild-type and 2AWC^{ON} animals. However, expression of NSY-1::GFP in the AWC cell body is faint in 2AWC^{ON} animals, suggesting that microtubules may be important for the stability of NSY-1 protein. These results suggest that the presence of wild-type levels of UNC-43 and NSY-1 in the AWC axons is dependent on microtubule function and is required for AWC asymmetry.

As *tir-1* promotes the synaptic localization of NSY-1 protein in the AWC axons (Chuang and Bargmann, 2005), reduced amounts of NSY-1 in the AWC axons of nocodazole-treated animals may be due to decreased TIR-1 localization in the axons. To determine whether the effect of nocodazole on the localization of UNC-43 in the AWC axons is dependent on reduced localization of TIR-1, the *odr-3p::unc-43::GFP* transgene was crossed to *tir-1(tm3036lf)* mutants. *tir-1(tm3036lf)*, probably a null allele, contains a deletion removing the C-terminal TIR activation domain and causing 100% of animals to become 2AWC^{ON} (Table 1, row p). The localization pattern and level of UNC-43::GFP in the AWC axons is similar in wild type and *tir-1(tm3036lf)* mutants (see Fig. S2 in the supplementary material), suggesting that UNC-43 localization in the AWC axons is regulated by microtubules but is independent of TIR-1 localization.

Together, these results are consistent with a model that microtubules are required for proper localization of TIR-1, UNC-43 and NSY-1 in the AWC axons to regulate the AWC^{OFF} cell identity.

The kinesin motor *unc-104/kif1a* genetically interacts with *tir-1* in the regulation of the AWC^{OFF} identity

Many proteins are transported by dynein/dynectin and kinesin motor proteins along microtubules to different locations within the cells (Muresan, 2000; Susalka et al., 2000). There are at least 25 dynein/dynectin-related and 23 kinesin-related genes predicted in the *C. elegans* genome (*C. elegans* Sequencing Consortium, 1998). To overcome potential functional redundancy of microtubule motor proteins in AWC asymmetry, we performed a sensitized RNA interference (RNAi) genetic screen using a *tir-1(ky388)* temperature-sensitive (ts) mutant, in which the 2AWC^{ON} phenotype was incompletely penetrant (34% 2AWC^{ON}) at 15°C (Chuang and Bargmann, 2005) (Table 2). We found that RNAi of the kinesin *unc-104* significantly enhanced the 2AWC^{ON} frequency from 34% to 58% in *tir-1(ky388ts)* at 15°C (Table 2; $P<0.001$). To confirm the effect of *unc-104(RNAi)* on AWC asymmetry, we made *tir-1(ky388ts); unc-104(e1265)* double mutants and found a strong enhancement of the 2AWC^{ON} frequency from 34% to 91% ($P<0.0001$). These results suggest that *unc-104* is required for the regulation of the AWC^{OFF} identity. *unc-104(RNAi)* or *unc-104(e1265)* alone did not show a 2AWC^{ON} phenotype. Single

DEVELOPMENT

Table 2. *unc-104/kif1a* genetically interacts with *tir-1* to regulate the AWC^{OFF} identity

Genetic background	2AWC^{OFF} (%)	1AWC^{OFF}/1AWC^{ON} (%)	2AWC^{ON} (%)	*n*
Wild type	1	99	0	110
tir-1(ky388ts)	0	66	34	151
tir-1(ky388ts); unc-104(RNAi)	0	42	58	106
tir-1(ky388ts); unc-104(e1265)	0	9	91	157
tir-1(ky388ts); unc-104(e1265); odr-3p::unc-104	4	57	39	105
unc-104(RNAi)	1	99	0	248
unc-104(e1265)	1	99	0	125
unc-104(rh142)	0	100	0	116
unc-104(rh43)	2	98	0	133

tir-1(ky388) temperature-sensitive (ts) mutants were grown at 15°C to maintain the low penetrance of 2AWC^{ON} phenotype.

mutants of more severe alleles *unc-104(rh43)* or *unc-104(rh142)* also did not cause 2AWC^{ON} (Table 2). These results suggest that *unc-104* may function redundantly with other microtubule motor proteins to regulate the AWC^{OFF} identity.

UNC-104 is localized adjacent to TIR-1 in the AWC axons

C. elegans unc-104 is widely expressed in the nervous system, including many unidentified head neurons (Zhou et al., 2001). To determine whether *unc-104* is expressed in AWC neurons, *unc-104p::GFP*, a GFP reporter transgene under the control of a 4.2 kb *unc-104* promoter, was co-expressed with the *odr-1p::DsRed* marker. The *unc-104p::GFP* transgene was expressed in many head neurons, including DsRed-labeled AWC neurons (Fig. 3A-C), suggesting that *unc-104* is expressed in AWC neurons.

We then expressed a tagged UNC-104::GFP fusion protein in the AWC neurons using the *odr-3* promoter and examined the subcellular localization of UNC-104. UNC-104::GFP was localized in a punctate pattern along the AWC axons and diffuse in the cell body (Fig. 3E). UNC-104::GFP and TIR-1::DsRed were not colocalized but were largely adjacent to each other in the AWC axons (Fig. 3F). The non-overlapping localization pattern of TIR-1 and UNC-104 in the AWC axons is consistent with the postsynaptic localization of TIR-1 protein compared with the role of *unc-104* in the transport of presynaptic vesicles (Chuang and Bargmann, 2005; Hall and Hedgecock, 1991).

unc-104/kif1a acts non-cell autonomously in the AWC^{ON} neuron to regulate the AWC^{OFF} identity

Expression of *unc-104* in AWC from the *odr-3* promoter significantly rescued the enhancement of 2AWC^{ON} frequency from 91% to 39% in *tir-1(ky388ts); unc-104(e1265)* double mutants (Table 2; $P<0.0001$). This result suggests that *unc-104* probably acts in AWC neurons to promote the AWC^{OFF} identity. To further refine the site of *unc-104* action in AWC asymmetry, mosaic animals in which *unc-104* activity is different between the two AWC neurons were used to determine whether *unc-104* acts in the AWC^{ON} cell, the AWC^{OFF} cell, or both. An extrachromosomal transgene containing *unc-104p::unc-104* and *odr-1p::DsRed* (expressed in AWC and AWB) was introduced into *unc-104(e1265)* mutants. The *unc-104p::unc-104* transgene rescued the uncoordinated locomotion phenotype of *unc-104(e1265)* mutants (data not shown). Transgenes expressing the *odr-1p::DsRed* marker and *unc-104p::unc-104* in both AWC neurons caused a mixed weak phenotype of 2AWC^{ON} and 2AWC^{OFF} (Fig. 4A). Spontaneous loss of the extrachromosomal array in one of the two AWC neurons resulted in mosaic animals in which one of the two AWC neurons expressed the transgene and therefore had *unc-104* activity; this cell could be identified by expression of the DsRed marker. In the majority of these mosaic animals, the *unc-104*(+) AWC neuron became AWC^{ON} and the *unc-104*(–) AWC neuron became AWC^{OFF} (Fig. 4B). These results are consistent with a significant cell-autonomous requirement for *unc-104* within the AWC^{ON} cell to regulate the AWC^{OFF} identity in a non-cell autonomous manner, which is different from the cell autonomous function of UNC-43, TIR-1 and NSY-1 in the regulation of AWC^{OFF} cell.

unc-104/kif1a is required for the localization of TIR-1, UNC-43, and NSY-1 in the AWC axons

C. elegans UNC-104 and the mouse ortholog K1F1A are neuron-specific kinesin motors that transport presynaptic vesicles along microtubules from the cell body to the nerve terminal (Hall and Hedgecock, 1991; Okada et al., 1995). In *unc-104(e1265)* mutants, most synaptic vesicles remain trapped in the cell body and are nearly absent from the axon (Hall and Hedgecock, 1991; Ou et al.,

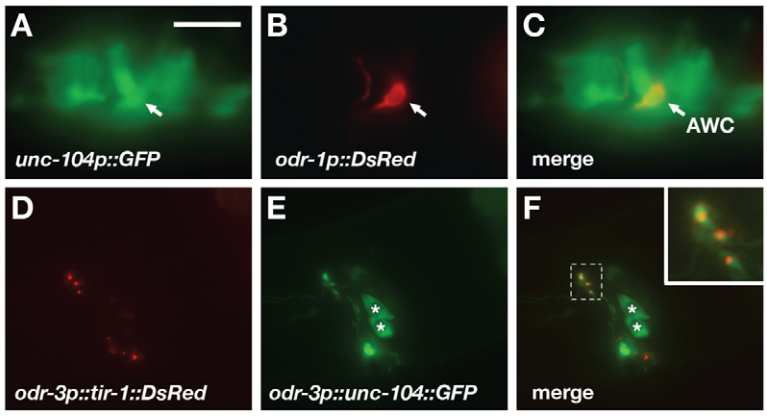

Fig. 3. UNC-104 is localized adjacent to TIR-1 in the AWC axons. (**A-C**) Images of *unc-104p::GFP* (A) and *odr-1p::DsRed* (B). Co-expression of GFP and DsRed in AWC appears yellow (C). Arrows indicate the cell body of AWC. (**D-F**) Images of TIR-1::DsRed (D) and UNC-104::GFP (E). UNC-104::GFP is localized adjacent to TIR-1::DsRed in AWC axons (F). Inset shows higher magnification of the area outlined. Scale bar: 10 μm.

DEVELOPMENT

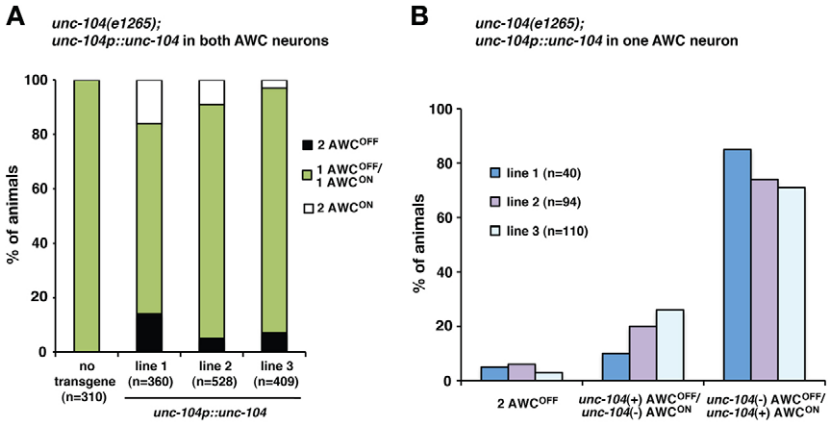

Fig. 4. *unc-104/kif1a* acts non-cell autonomously in AWC^{ON} to specify AWC^{OFF} fate. (**A**,**B**) AWC phenotypes of *unc-104(e1265)* mutants expressing the transgene *unc-104p::unc-104; odr-1p::DsRed* in both AWC neurons (A) or in one of the two AWC neurons (B).

2010). UNC-49 GABA receptors form postsynaptic clusters at neuromuscular junctions in a *unc-104*-dependent manner, suggesting that a factor required for postsynaptic receptor clustering is transported from the cell body to presynaptic sites by UNC-104 (Gally and Bessereau, 2003).

To determine whether the postsynaptic localization of TIR-1, like postsynaptic GABA receptors, is dependent on *unc-104*, we quantitatively analyzed the localization pattern of TIR-1::GFP in wild-type animals and *unc-104* mutants. The intensities of TIR-1::GFP puncta were significantly different between wild-type and *unc-104(e1265)* mutant animals. TIR-1::GFP puncta in the AWC axons were bright in wild-type animals but were faint in *unc-104* mutants (Fig. 5A-C; $P<0.0001$), suggesting that only a small fraction of TIR-l was localized to puncta in the AWC axons in *unc-104(e1265)* mutants compared with wild type. Unlike synaptic vesicles, dense core vesicles and UNC-6/netrin [which were shown to accumulate in the cell body and dendrites of *unc-104* mutants (Asakura et al., 2010; Hall and Hedgecock, 1991; Nonet, 1999; Ou et al., 2010; Zahn et al., 2004)], TIR-1 was not detected in the AWC cell body or dendrites in *unc-104* mutants. These results suggest that *unc-104* may be required for the stability of TIR-1 protein, similar to the function of kinesin KIF4 in regulating intracellular trafficking and stability of HIV-1 Gag polyprotein (Martinez et al., 2008). To rule out the possibility that the *odr-3* promoter is downregulated in *unc-104(e1265)* mutants, the expression level of *odr-3p::GFP* was examined in wild-type and *unc-104(e1265)* mutants. The expression level of *odr-3p::GFP* in the AWC cell body is not significantly different between wild-type animals and *unc-104(e1265)* mutants (see Fig. S3 in the supplementary material), suggesting that the *odr-3* promoter is not regulated by *unc-104*. These results support the hypothesis that UNC-104 may transport some presynaptic factors that regulate the localization of TIR-1 to the postsynaptic sites of the AWC axons, and may also regulate the stability of TIR-1 protein.

To examine whether TIR-1 is dynamically transported in the AWC cell in a manner dependent on *unc-104*, we imaged TIR-1::GFP in the AWC axons of L1 animals using a highly sensitive CCD camera. Time-lapse imaging revealed that some stable TIR-1::GFP puncta gave rise to mobile puncta, which then moved rapidly toward the distal axon (anterograde) or towards the cell body (retrograde) (Fig. 6A,B). In wild-type animals, moving TIR-1::GFP trafficked in the anterograde direction in 55% of observed events and in the retrograde direction in 45% of observed events. In *unc-104(e1265)* mutants, the ratio of anterograde movement was significantly reduced to 33% and the ratio of retrograde movement was significantly increased to 67% (Fig. 6C; $P<0.001$). These results suggest that the motor protein, if any, directly required for the anterograde movement of TIR-1 in the AWC axons is partly dependent on *unc-104* activity, and that anterograde and retrograde transport of TIR-1 is regulated differently. We also measured the velocities of anterograde and retrograde movements of TIR-1::GFP. In wild-type animals, the average speed of anterograde movements is 1.8 μm/second, similar to the speed of *unc-104*-dependent movements of synaptic vesicles precursors and dense core vesicles measured from in vivo imaging of *C. elegans* neurons (Ou et al., 2010; Zahn et al., 2004). The average speed of retrograde

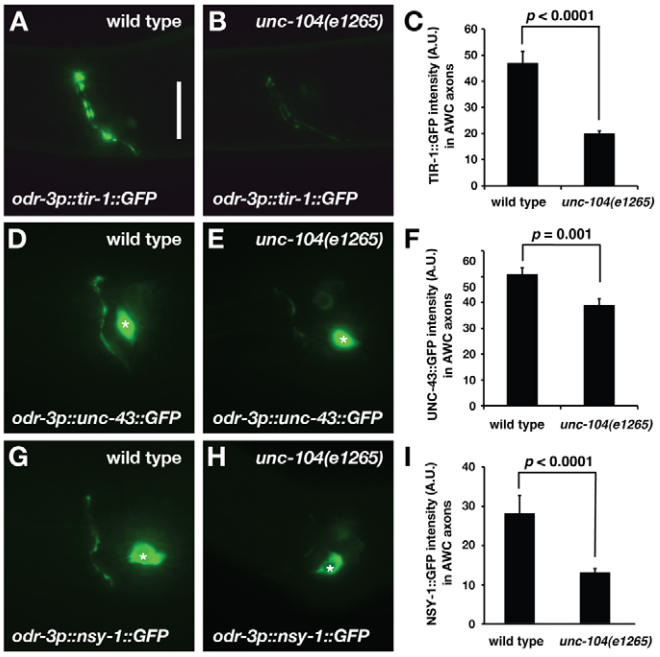

Fig. 5. The kinesin motor *unc-104/kif1a* is required for the localization of TIR-1, UNC-43 and NSY-1 in the AWC axons. (**A**,**B**) Localization of TIR-1::GFP in AWC neurons of wild-type (A) and *unc-104(e1265)* (B). (**C**) The average intensity of TIR-1::GFP in the AWC axons. (**D**,**E**) Localization of UNC-43::GFP in AWC neurons of wild-type (D) and *unc-104(e1265)* (E). (**F**) The average intensity of UNC-43::GFP in AWC axons. (**G**,**H**) Localization of NSY-1::GFP in AWC neurons of wild-type (G) and *unc-104(e1265)* (H). (**I**) The average intensity of NSY-1::GFP in AWC axons. Images were taken from L1 animals. Asterisks indicate cell bodies. Scale bar: 10 μm. A.U., arbitrary unit. Error bars indicate the s.e.m.; *t*-test; $n=20$ for each transgene per genotype in C,F,I.

DEVELOPMENT

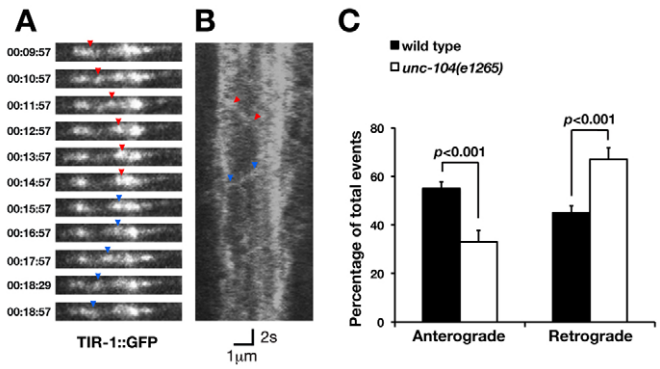

Fig. 6. Dynamic trafficking of TIR-1 in the AWC axons is dependent on *unc-104/kif1a*. (**A**) Representative images of moving TIR-1::GFP puncta in wild-type AWC axons. Red arrowheads indicate retrogradely moving puncta and blue arrowheads indicate anterogradely moving puncta. (**B**) Kymograph of the movie shown in A. The speed of the retrograde movement within the two red arrowheads is 1.2 μm/second; the speed of the anterograde movement between the two blue arrowheads is 1.9 μm/second. (**C**) The percentage of anterograde and retrograde trafficking events. *n*=314 and *n*=101 trafficking events in wild type and *unc-104(e1265)*, respectively. Error bars indicate the s.e.m. *Z*-test for two proportions.

movements is 1.7 μm/seconds, similar to the speed of the retrograde motor dynein in living *Dictyostelium* cells (Ma and Chisholm, 2002). The average speed of TIR-1 movement in either direction was not significantly altered in *unc-104(e1265)* mutants (data not shown). These results suggest that altered localization of TIR-1 is dependent on changes in the average direction, rather than the average speed, of transport.

As the localization of UNC-43 and NSY-1, like TIR-1, in the AWC axons was significantly reduced in nocodazole-induced 2AWC^{ON} animals, we also examined the possibility that the localization of these proteins could be regulated by *unc-104*. In *unc-104(e1265)* mutants, UNC-43::GFP and NSY-1::GFP showed significantly reduced levels of localization in the AWC axons (Fig. 5D-I). Like the effect of nocodazole on their localization in 2AWC^{ON} animals (Fig. 2D-I), the expression level of UNC-43::GFP in the AWC cell body was similar in wild type and *unc-104(e1265)* mutants, whereas NSY-1::GFP expression was reduced in the AWC cell body in *unc-104(e1265)* mutants. These results suggest that *unc-104* is required for the localization and/or stabilization of UNC-43 and NSY-1 in the AWC axons.

DISCUSSION

One challenge for genetic approaches aimed at studying biological processes is the difficulty of identifying specific functions for broadly acting cell biological pathways. Here, we complement classical genetics with a chemical approach to disrupt polymerized microtubules at a specific time in development. Complete microtubule loss leads to lethality and defects in mitosis, but our experiments took advantage of the fact that late embryogenesis, the time at which asymmetric AWC identities are determined, is a time when little cell division occurs. Using a combination of genetics and drug treatment, we have linked microtubule-dependent localization of calcium-regulated signaling proteins, including UNC-43/CaMKII, TIR-1/SARM adaptor and NSY-1/ASK1 MAPKKK to genetic control of neuronal asymmetry in *C. elegans*. We also identified the requirement of microtubule-dependent kinesin motor gene *unc-104/kif1a* in this process.

Our results suggest that microtubule-dependent and *unc-104*-dependent localization of the TIR-1 signaling complex in the AWC axons may be required for maintenance of AWC asymmetry in early larval stages. In addition, the requirement of nocodazole treatment in embryos for generating AWC phenotypes and the potential role of *unc-104* in a negative feedback signal from pre-AWC^{ON} to pre-AWC^{OFF} suggest that microtubules and *unc-104* may also function in the early AWC^{ON}/AWC^{OFF} decision step during embryogenesis.

Nocodazole needs to be present before and/or during the crucial period in late embryos to affect AWC asymmetry. Two hours of nocodazole treatment would be sufficient to allow the drug to penetrate the embryos. Although the exposure of embryos to nocodazole is transient, the retention of nocodazole in treated early embryos could continue to inhibit microtubule function and microtubule-dependent assembly of the UNC-43/TIR-1/NSY-1 signaling complex in the AWC axons until the crucial stage of AWC asymmetry in late embryos and the maintenance of asymmetry in early larvae. Alternatively, nocodazole may only affect the process in the embryos, and the effect of the drug is then stabilized though the maintenance pathway.

TIR-1 is dynamically transported in both anterograde and retrograde directions in the AWC axons. Analogous to retrograde neurotrophin signaling (Ginty and Segal, 2002), lateral signaling between AWC neurons may be transmitted in a retrograde direction from the synapses to the cell body to regulate distinct patterns of gene expression. It is possible that TIR-1 may serve as an adaptor to link some yet to be identified motor proteins and the UNC-43/TIR-1/NSY-1 calcium-signaling complex for both anterograde and retrograde transport of signals that regulate asymmetric AWC gene expression. Microtubule depolymerization by nocodazole results in defective AWC asymmetry, which could be due to disruption of both anterograde and retrograde transport of the TIR-1 signaling complex. The identification of microtubule-dependent kinesin motor gene *unc-104* in this process will lay the groundwork for future studies of the genetic networks that link microtubules and the regulation of calcium signaling in stochastic left-right neuronal asymmetry.

The localization of UNC-43, TIR-1 and NSY-1 to the AWC axons was significantly reduced in *unc-104(e1265lf)* mutants, although the reduced level of these calcium signaling proteins was probably sufficient to regulate AWC asymmetry as *unc-104(e1265lf)* single mutants did not have 2AWC^{ON} phenotype. *unc-104* may function redundantly with other unknown motor proteins or microtubule components to regulate the AWC^{OFF} identity. Functional redundancy of different motor proteins has been shown for assembly of the mitotic spindle and transport of mitochondria (Nag et al., 2008; Nangaku et al., 1994; Roof et al., 1992; Tanaka et al., 1998). In *tir-1(ky388ts); unc-104(e1265lf)* double mutants, a strong enhancement of the 2AWC^{ON} phenotype could be due to a synergistic effect of reduced *tir-1* activity in *tir-1(ky388ts)* mutants and decreased localization of the UNC-43/TIR-1/NSY-1 signaling complex in the AWC axons of *unc-104(e1265lf)* mutants.

UNC-43, TIR-1 and NSY-1 are enriched at postsynaptic sites of the AWC axons (Chuang and Bargmann, 2005), and their localization in the AWC axons is dependent on *unc-104*, which has been previously shown to transport presynaptic vesicles along microtubules from the cell body to the nerve terminal (Hall and Hedgecock, 1991; Okada et al., 1995). UNC-104/KIF1A may transport some presynaptic factor(s) in the future AWC^{ON} cell that non-cell autonomously regulate the trafficking of UNC-43/TIR-

DEVELOPMENT

1/NSY-1 signaling complexes to postsynaptic regions of the AWC axons to regulate the AWC^{OFF} identity. *ccy-1* (cyclin), *pct-1* (cyclin-dependent Pctaire kinase) and *cdk-5* (cyclin-dependent kinase) are part of the two cyclin-dependent pathways that act in parallel and partially redundantly to direct polarized trafficking of presynaptic components. *unc-104* might be involved in the same biological processes as both cyclin-dependent pathways (Ou et al., 2010). Our results showed that *ccy-1(RNAi)* and *pct-1(RNAi)*, but not *cdk-5(RNAi)*, significantly enhanced the $2AWC^{ON}$ phenotype of *tir-1(ky388ts)* mutants. However, *ccy-1(RNAi); unc-104(e1265lf)* or *pct-1(RNAi); unc-104(e1265lf)* did not show AWC phenotypes (data not shown). These results suggest that *ccy-1, pct-1* and *unc-104* may act in the same pathway to transport presynaptic factors that regulate the postsynaptic localization of the TIR-1 signaling complex in the AWC axons. A loss-of-function mutation in *unc-13*, which encodes a novel conserved protein that regulates neurotransmitter release at the synapse (Maruyama and Brenner, 1991), did not enhance the $2AWC^{ON}$ phenotype of *tir-1(ky388ts)* mutants (data not shown). It is possible that *unc-13(e450lf)* mutants may still have residual neurotransmission activity. Alternatively, the presynaptic factors regulating the trafficking of UNC-43/TIR-1/NSY-1 in the AWC axons could be non-vesicular proteins transported by the kinesin UNC-104.

NSY-5 gap junctions and NSY-4 claudins are two parallel signaling systems that have opposite intrinsic side biases to induce the AWC^{ON} state. It has been proposed that stochastic AWC asymmetry may be driven by relative strengths of the *nsy-5* signal and the *nsy-4* signal when the two AWC neurons communicate through the NSY-5 gap junction neuronal network. The AWC cell with a stronger signal then generates a negative-feedback signal to suppress the AWC^{ON} state in the contralateral AWC (Chuang et al., 2007). However, the molecular mechanisms of this negative-feedback regulation are not understood. Our genetic results suggest that *unc-104* may function cell-autonomously in the pre-AWC^{ON} cell through an unknown mechanism to regulate the AWC^{ON} identity. In addition, *unc-104* may non-cell autonomously control the localization of UNC-43, TIR-1 and NSY-1 in the pre-AWC^{OFF} cell to regulate the AWC^{OFF} identity, distinct from the cell-autonomous activity of the TIR-1 signaling complex required in the AWC^{OFF} cell. We propose that *unc-104* may be involved in a negative-feedback signal, sent from pre-AWC^{ON} to pre-AWC^{OFF}, to ensure enactment of a precise AWC^{ON}/AWC^{OFF} decision. Identification and characterization of the presynaptic factors transported by UNC-104 would shed light on such negative-feedback mechanisms.

Microtubules have been implicated in different biological processes of the developing nervous system, including neurogenesis, neuronal migration, axon guidance and synapse formation (Singh and Tsai, 2010). Mutations in human tubulin genes or in genes that regulate microtubule function give rise to brain disorders (Demer et al., 2005; des Portes et al., 1998; Gleeson et al., 1998; Jaglin et al., 2009; Keays et al., 2007; Poirier et al., 2007; Tischfield et al., 2010). In addition, dysfunction of microtubule-motor-dependent axonal transport has been linked to several neurodegenerative diseases (De Vos et al., 2008). This study reveals specific roles of microtubules and microtubule-dependent kinesin motor *unc-104/kif1a* in regulating calcium signaling for asymmetric neuronal differentiation.

TIR-1 is an ortholog of the mammalian TIR domain adaptor protein SARM (Mink et al., 2001), which is also called MyD88-5 (Kim et al., 2007). SARM is expressed primarily in neurons, and associates with microtubules and mitochondria, as well as JNK3 and MAPK10 isoform 3. Hippocampal neurons from SARM-deficient mice are protected from death during deprivation of oxygen and glucose, suggesting an important role for SARM in regulating neuronal survival (Kim et al., 2007). TIR-1 and NSY-1 are implicated in regulation of anoxic death (Hayakawa et al., 2011), suggesting that this pathway may also have a conserved function in neuronal survival in response to stress. In addition, SARM regulates microtubule stability and neuronal morphology (Chen et al., 2011). Our study of microtubules and motor proteins in trafficking of the TIR-1 calcium-signaling complex in the context of neuronal differentiation and function may provide insights into the regulation of SARM function and calcium signaling in other aspects of neural development.

Acknowledgements
We thank Eun Chae, Shunyan Weng, Felicia Ciamacco, Brittany Bayne and Kalyn Campbell for technical assistance; Yan Zou for worm cDNA; Celine Maeder and Kang Shen for the advice of time lapse imaging; and Vaughn Cleghon and Jim Wells for comments on the manuscript. We also thank Andy Fire for *C. elegans* vectors; Theresa Stiernagle and the *C. elegans* Genetic Center for *C. elegans* strains; Shohei Mitani for *tir-1(tm3036)*; and the WormBase. This work was supported by Whitehall Foundation Research Awards (C.C. and C.-F.C.), by the March of Dimes Foundation (C.C.), by an Alfred P. Sloan Research Fellowship (C.-F.C.) and by a NIH Training Grant of Organogenesis (Y.-W.H.). C.I.B. is an investigator of the Howard Hughes Medical Institute. Deposited in PMC for release after 6 months.

Competing interests statement
The authors declare no competing financial interests.

Supplementary material
Supplementary material for this article is available at
http://dev.biologists.org/lookup/suppl/doi:10.1242/dev.069740/-/DC1

References

Abe, T., Thitamadee, S. and Hashimoto, T. (2004). Microtubule defects and cell morphogenesis in the lefty1lefty2 tubulin mutant of Arabidopsis thaliana. *Plant Cell Physiol.* **45**, 211-220.
Asakura, T., Waga, N., Ogura, K. and Goshima, Y. (2010). Genes required for cellular UNC-6/netrin localization in *Caenorhabditis elegans*. *Genetics* **185**, 573-585.
Bauer Huang, S. L., Saheki, Y., VanHoven, M. K., Torayama, I., Ishihara, T., Katsura, I., van der Linden, A., Sengupta, P. and Bargmann, C. I. (2007). Left-right olfactory asymmetry results from antagonistic functions of voltage-activated calcium channels and the Raw repeat protein OLRN-1 in C. elegans. *Neural Dev.* **2**, 24.
Brenner, S. (1974). The genetics of *Caenorhabditis elegans*. *Genetics* **77**, 71-94.
***C. elegans* Sequencing Consortium** (1998). Genome sequence of the nematode *C. elegans*: a platform for investigating biology. *Science* **282**, 2012-2018.
Chang, S., Johnston, R. J., Jr and Hobert, O. (2003). A transcriptional regulatory cascade that controls left/right asymmetry in chemosensory neurons of *C. elegans*. *Genes Dev.* **17**, 2123-2137.
Chen, C. Y., Lin, C. W., Chang, C. Y., Jiang, S. T. and Hsueh, Y. P. (2011). Sarm1, a negative regulator of innate immunity, interacts with syndecan-2 and regulates neuronal morphology. *J. Cell Biol.* **193**, 769-784.
Chuang, C. F. and Bargmann, C. I. (2005). A Toll-interleukin 1 repeat protein at the synapse specifies asymmetric odorant receptor expression via ASK1 MAPKKK signaling. *Genes Dev.* **19**, 270-281.
Chuang, C. F., Vanhoven, M. K., Fetter, R. D., Verselis, V. K. and Bargmann, C. I. (2007). An innexin-dependent cell network establishes left-right neuronal asymmetry in *C. elegans*. *Cell* **129**, 787-799.
De Vos, K. J., Grierson, A. J., Ackerley, S. and Miller, C. C. (2008). Role of axonal transport in neurodegenerative diseases. *Annu. Rev. Neurosci.* **31**, 151-173.
Demer, J. L., Clark, R. A. and Engle, E. C. (2005). Magnetic resonance imaging evidence for widespread orbital dysinnervation in congenital fibrosis of extraocular muscles due to mutations in KIF21A. *Invest. Ophthalmol. Vis. Sci.* **46**, 530-539.
des Portes, V., Pinard, J. M., Billuart, P., Vinet, M. C., Koulakoff, A., Carrie, A., Gelot, A., Dupuis, E., Motte, J., Berwald-Netter, Y. et al. (1998). A novel CNS gene required for neuronal migration and involved in X-linked subcortical laminar heterotopia and lissencephaly syndrome. *Cell* **92**, 51-61.
Driscoll, M., Dean, E., Reilly, E., Bergholz, E. and Chalfie, M. (1989). Genetic and molecular analysis of a *Caenorhabditis elegans* beta-tubulin that conveys benzimidazole sensitivity. *J. Cell Biol.* **109**, 2993-3003.

Gally, C. and Bessereau, J. L. (2003). GABA is dispensable for the formation of junctional GABA receptor clusters in *Caenorhabditis elegans*. *J. Neurosci.* **23**, 2591-2599.
Ginty, D. D. and Segal, R. A. (2002). Retrograde neurotrophin signaling: Trk-ing along the axon. *Curr. Opin. Neurobiol.* **12**, 268-274.
Gleeson, J. G., Allen, K. M., Fox, J. W., Lamperti, E. D., Berkovic, S., Scheffer, I., Cooper, E. C., Dobyns, W. B., Minnerath, S. R., Ross, M. E. et al. (1998). Doublecortin, a brain-specific gene mutated in human X-linked lissencephaly and double cortex syndrome, encodes a putative signaling protein. *Cell* **92**, 63-72.
Hall, D. H. and Hedgecock, E. M. (1991). Kinesin-related gene unc-104 is required for axonal transport of synaptic vesicles in *C. elegans*. *Cell* **65**, 837-847.
Hayakawa, T., Kato, K., Hayakawa, R., Hisamoto, N., Matsumoto, K., Takeda, K. and Ichijo, H. (2011). Regulation of anoxic death in *Caenorhabditis elegans* by mammalian apoptosis signal-regulating kinase (ASK) family proteins. *Genetics* **187**, 785-792.
Hobert, O. (2006). Architecture of a microRNA-controlled gene regulatory network that diversifies neuronal cell fates. *Cold Spring Harb. Symp. Quant. Biol.* **71**, 181-188.
Hobert, O., Johnston, R. J., Jr and Chang, S. (2002). Left-right asymmetry in the nervous system: the *Caenorhabditis elegans* model. *Nat. Rev. Neurosci.* **3**, 629-640.
Jaglin, X. H., Poirier, K., Saillour, Y., Buhler, E., Tian, G., Bahi-Buisson, N., Fallet-Bianco, C., Phan-Dinh-Tuy, F., Kong, X. P., Bomont, P. et al. (2009). Mutations in the beta-tubulin gene TUBB2B result in asymmetrical polymicrogyria. *Nat. Genet.* **41**, 746-752.
Keays, D. A., Tian, G., Poirier, K., Huang, G. J., Siebold, C., Cleak, J., Oliver, P. L., Fray, M., Harvey, R. J., Molnar, Z. et al. (2007). Mutations in alpha-tubulin cause abnormal neuronal migration in mice and lissencephaly in humans. *Cell* **128**, 45-57.
Kim, Y., Zhou, P., Qian, L., Chuang, J. Z., Lee, J., Li, C., Iadecola, C., Nathan, C. and Ding, A. (2007). MyD88-5 links mitochondria, microtubules, and JNK3 in neurons and regulates neuronal survival. *J. Exp. Med.* **204**, 2063-2074.
Koga, M. and Ohshima, Y. (2004). The *C. elegans* ceh-36 gene encodes a putative homemodomain transcription factor involved in chemosensory functions of ASE and AWC neurons. *J. Mol. Biol.* **336**, 579-587.
Lanjuin, A., VanHoven, M. K., Bargmann, C. I., Thompson, J. K. and Sengupta, P. (2003). Otx/otd homeobox genes specify distinct sensory neuron identities in *C. elegans*. *Dev. Cell* **5**, 621-633.
Lesch, B. J. and Bargmann, C. I. (2010). The homeodomain protein hmbx-1 maintains asymmetric gene expression in adult *C. elegans* olfactory neurons. *Genes Dev.* **24**, 1802-1815.
Lesch, B. J., Gehrke, A. R., Bulyk, M. L. and Bargmann, C. I. (2009). Transcriptional regulation and stabilization of left-right neuronal identity in *C. elegans*. *Genes Dev.* **23**, 345-358.
Levin, M. and Palmer, A. R. (2007). Left-right patterning from the inside out: widespread evidence for intracellular control. *BioEssays* **29**, 271-287.
Lu, C., Srayko, M. and Mains, P. E. (2004). The *Caenorhabditis elegans* microtubule-severing complex MEI-1/MEI-2 katanin interacts differently with two superficially redundant beta-tubulin isotypes. *Mol. Biol. Cell* **15**, 142-150.
Ma, S. and Chisholm, R. L. (2002). Cytoplasmic dynein-associated structures move bidirectionally in vivo. *J. Cell Sci.* **115**, 1453-1460.
Martinez, N. W., Xue, X., Berro, R. G., Kreitzer, G. and Resh, M. D. (2008). Kinesin KIF4 regulates intracellular trafficking and stability of the human immunodeficiency virus type 1 Gag polyprotein. *J. Virol.* **82**, 9937-9950.
Maruyama, I. N. and Brenner, S. (1991). A phorbol ester/diacylglycerol-binding protein encoded by the unc-13 gene of *Caenorhabditis elegans*. *Proc. Natl. Acad. Sci. USA* **88**, 5729-5733.
Mello, C. and Fire, A. (1995). DNA transformation. *Methods Cell Biol.* **48**, 451-482.
Mink, M., Fogelgren, B., Olszewski, K., Maroy, P. and Csiszar, K. (2001). A novel human gene (SARM) at chromosome 17q11 encodes a protein with a SAM motif and structural similarity to Armadillo/beta-catenin that is conserved in mouse, *Drosophila*, and *Caenorhabditis elegans*. *Genomics* **74**, 234-244.
Muresan, V. (2000). One axon, many kinesins: what's the logic? *J. Neurocytol.* **29**, 799-818.
Nag, D. K., Tikhonenko, I., Soga, I. and Koonce, M. P. (2008). Disruption of four kinesin genes in dictyostelium. *BMC Cell Biol.* **9**, 21.
Nangaku, M., Sato-Yoshitake, R., Okada, Y., Noda, Y., Takemura, R., Yamazaki, H. and Hirokawa, N. (1994). KIF1B, a novel microtubule plus end-directed monomeric motor protein for transport of mitochondria. *Cell* **79**, 1209-1220.
Nonaka, S., Tanaka, Y., Okada, Y., Takeda, S., Harada, A., Kanai, Y., Kido, M. and Hirokawa, N. (1998). Randomization of left-right asymmetry due to loss of nodal cilia generating leftward flow of extraembryonic fluid in mice lacking KIF3B motor protein. *Cell* **95**, 829-837.
Nonet, M. L. (1999). Visualization of synaptic specializations in live *C. elegans* with synaptic vesicle protein-GFP fusions. *J. Neurosci. Methods* **89**, 33-40.
Okada, Y., Yamazaki, H., Sekine-Aizawa, Y. and Hirokawa, N. (1995). The neuron-specific kinesin superfamily protein KIF1A is a unique monomeric motor for anterograde axonal transport of synaptic vesicle precursors. *Cell* **81**, 769-780.
Ou, C. Y., Poon, V. Y., Maeder, C. I., Watanabe, S., Lehrman, E. K., Fu, A. K., Park, M., Fu, W. Y., Jorgensen, E. M., Ip, N. Y. et al. (2010). Two cyclin-dependent kinase pathways are essential for polarized trafficking of presynaptic components. *Cell* **141**, 846-858.
Phillips, J. B., Lyczak, R., Ellis, G. C. and Bowerman, B. (2004). Roles for two partially redundant alpha-tubulins during mitosis in early *Caenorhabditis elegans* embryos. *Cell Motil. Cytoskeleton* **58**, 112-126.
Pierce-Shimomura, J. T., Faumont, S., Gaston, M. R., Pearson, B. J. and Lockery, S. R. (2001). The homeobox gene lim-6 is required for distinct chemosensory representations in *C. elegans*. *Nature* **410**, 694-698.
Poirier, K., Keays, D. A., Francis, F., Saillour, Y., Bahi, N., Manouvrier, S., Fallet-Bianco, C., Pasquier, L., Toutain, A., Tuy, F. P. et al. (2007). Large spectrum of lissencephaly and pachygyria phenotypes resulting from de novo missense mutations in tubulin alpha 1A (TUBA1A). *Hum. Mutat.* **28**, 1055-1064.
Poole, R. J. and Hobert, O. (2006). Early embryonic programming of neuronal left/right asymmetry in *C. elegans*. *Curr. Biol.* **16**, 2279-2292.
Roayaie, K., Crump, J. G., Sagasti, A. and Bargmann, C. I. (1998). The G alpha protein ODR-3 mediates olfactory and nociceptive function and controls cilium morphogenesis in *C. elegans* olfactory neurons. *Neuron* **20**, 55-67.
Roof, D. M., Meluh, P. B. and Rose, M. D. (1992). Kinesin-related proteins required for assembly of the mitotic spindle. *J. Cell Biol.* **118**, 95-108.
Sagasti, A., Hisamoto, N., Hyodo, J., Tanaka-Hino, M., Matsumoto, K. and Bargmann, C. I. (2001). The CaMKII UNC-43 activates the MAPKKK NSY-1 to execute a lateral signaling decision required for asymmetric olfactory neuron fates. *Cell* **105**, 221-232.
Singh, K. K. and Tsai, L. H. (2010). MicroTUB(B3)ules and brain development. *Cell* **140**, 30-32.
Supp, D. M., Witte, D. P., Potter, S. S. and Brueckner, M. (1997). Mutation of an axonemal dynein affects left-right asymmetry in inversus viscerum mice. *Nature* **389**, 963-966.
Susalka, S. J., Hancock, W. O. and Pfister, K. K. (2000). Distinct cytoplasmic dynein complexes are transported by different mechanisms in axons. *Biochim. Biophys. Acta* **1496**, 76-88.
Takeda, S., Yonekawa, Y., Tanaka, Y., Okada, Y., Nonaka, S. and Hirokawa, N. (1999). Left-right asymmetry and kinesin superfamily protein KIF3A: new insights in determination of laterality and mesoderm induction by kif3A–/– mice analysis. *J. Cell Biol.* **145**, 825-836.
Tanaka, Y., Kanai, Y., Okada, Y., Nonaka, S., Takeda, S., Harada, A. and Hirokawa, N. (1998). Targeted disruption of mouse conventional kinesin heavy chain, kif5B, results in abnormal perinuclear clustering of mitochondria. *Cell* **93**, 1147-1158.
Tanaka-Hino, M., Sagasti, A., Hisamoto, N., Kawasaki, M., Nakano, S., Ninomiya-Tsuji, J., Bargmann, C. I. and Matsumoto, K. (2002). SEK-1 MAPKK mediates Ca2+ signaling to determine neuronal asymmetric development in *Caenorhabditis elegans*. *EMBO Rep.* **3**, 56-62.
Taylor, R. W., Hsieh, Y. W., Gamse, J. T. and Chuang, C. F. (2010). Making a difference together: reciprocal interactions in *C. elegans* and zebrafish asymmetric neural development. *Development* **137**, 681-691.
Thitamadee, S., Tuchihara, K. and Hashimoto, T. (2002). Microtubule basis for left-handed helical growth in *Arabidopsis*. *Nature* **417**, 193-196.
Tischfield, M. A., Baris, H. N., Wu, C., Rudolph, G., Van Maldergem, L., He, W., Chan, W. M., Andrews, C., Demer, J. L., Robertson, R. L. et al. (2010). Human TUBB3 mutations perturb microtubule dynamics, kinesin interactions, and axon guidance. *Cell* **140**, 74-87.
Troemel, E. R., Sagasti, A. and Bargmann, C. I. (1999). Lateral signaling mediated by axon contact and calcium entry regulates asymmetric odorant receptor expression in *C. elegans*. *Cell* **99**, 387-398.
VanHoven, M. K., Bauer Huang, S. L., Albin, S. D. and Bargmann, C. I. (2006). The claudin superfamily protein nsy-4 biases lateral signaling to generate left-right asymmetry in *C. elegans* olfactory neurons. *Neuron* **51**, 291-302.
Wes, P. D. and Bargmann, C. I. (2001). *C. elegans* odour discrimination requires asymmetric diversity in olfactory neurons. *Nature* **410**, 698-701.
White, J. G., Southgate, E., Thomson, J. N. and Brenner, S. (1986). The structure of the nervous system of *Caenorhabditis elegans*. *Philos. Trans. R. Soc. Lond.* B *Biol. Sci.* **314**, 1-340.
Wright, A. J. and Hunter, C. P. (2003). Mutations in a beta-tubulin disrupt spindle orientation and microtubule dynamics in the early *Caenorhabditis elegans* embryo. *Mol. Biol. Cell* **14**, 4512-4525.
Yu, S., Avery, L., Baude, E. and Garbers, D. L. (1997). Guanylyl cyclase expression in specific sensory neurons: a new family of chemosensory receptors. *Proc. Natl. Acad. Sci. USA* **94**, 3384-3387.
Zahn, T. R., Angleson, J. K., MacMorris, M. A., Domke, E., Hutton, J. F., Schwartz, C. and Hutton, J. C. (2004). Dense core vesicle dynamics in *Caenorhabditis elegans* neurons and the role of kinesin UNC-104. *Traffic* **5**, 544-559.
Zhou, H. M., Brust-Mascher, I. and Scholey, J. M. (2001). Direct visualization of the movement of the monomeric axonal transport motor UNC-104 along neuronal processes in living *Caenorhabditis elegans*. *J. Neurosci.* **21**, 3749-3755.

DEVELOPMENT

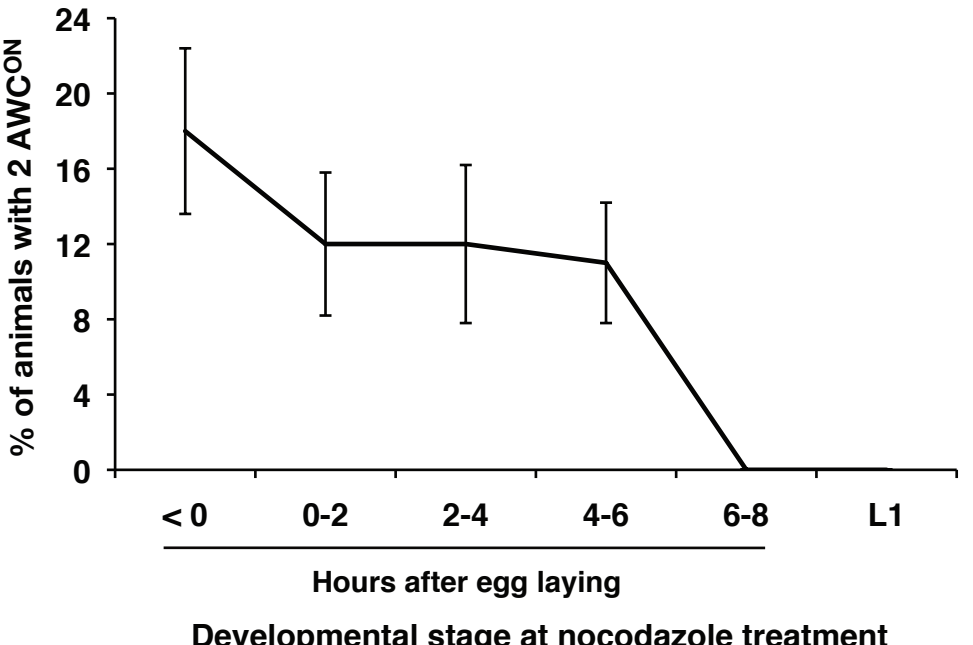
% of animals with 2 AWC^{ON}
24
20
16
12
8
4
0
< 0
0-2
2-4
4-6
6-8
L1
Hours after egg laying
Developmental stage at nocodazole treatment

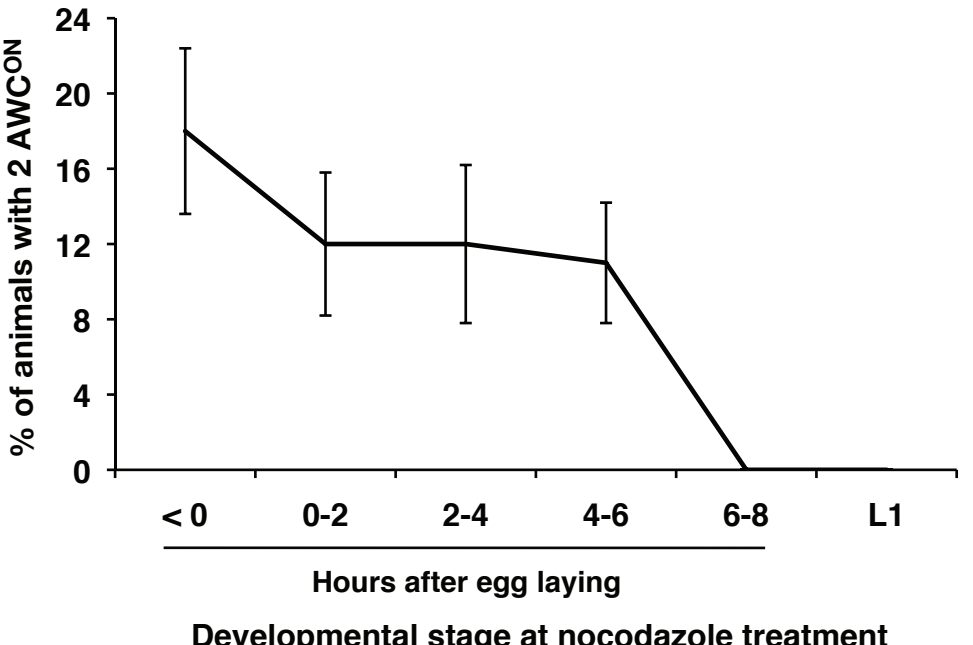
% of animals with 2 AWC^{ON}
24
20
16
12
8
4
0
< 0
0-2
2-4
4-6
6-8
L1
Hours after egg laying
Developmental stage at nocodazole treatment

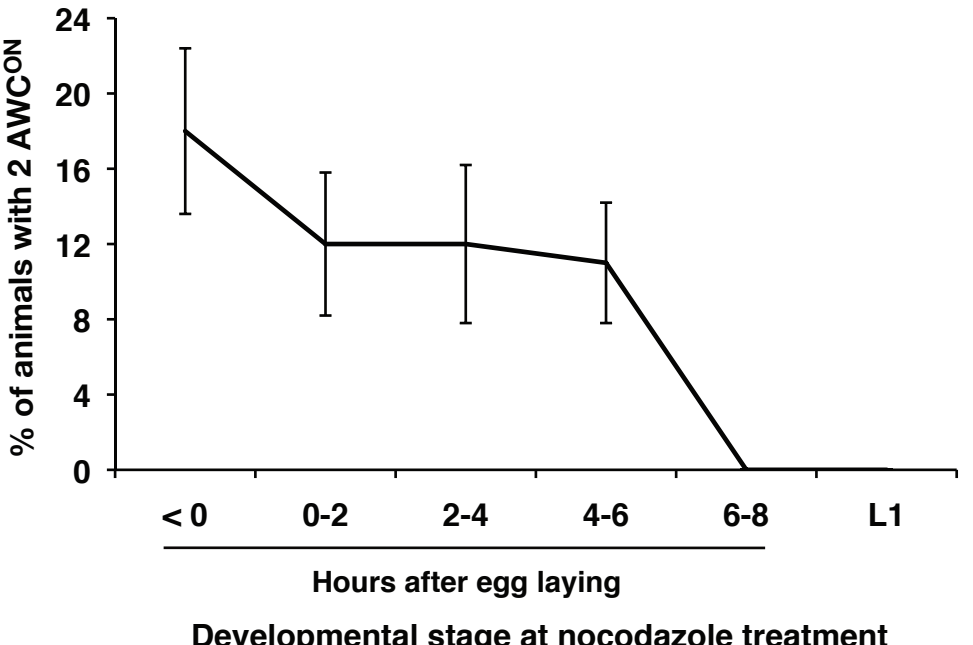
% of animals with 2 AWC^{ON}
24
20
16
12
8
4
0
< 0
0-2
2-4
4-6
6-8
L1
Hours after egg laying
Developmental stage at nocodazole treatment

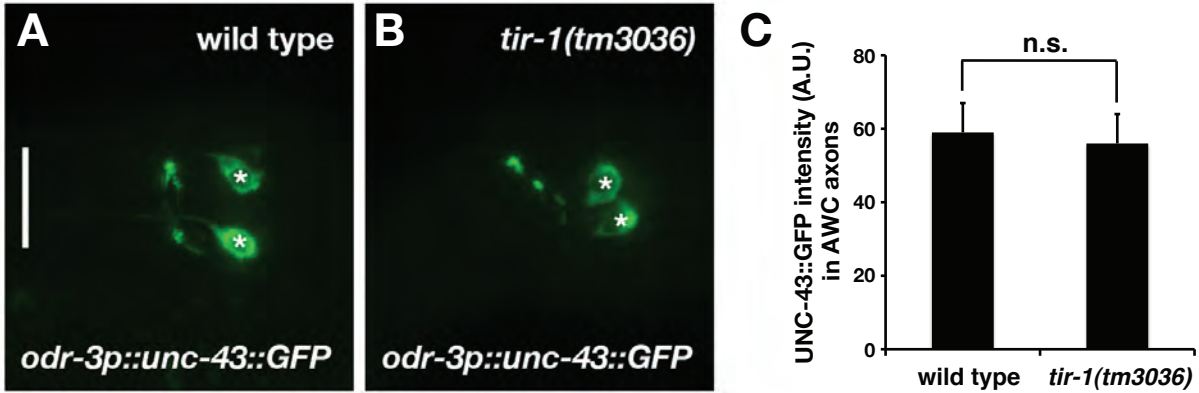
A
wild type
odr-3p::unc-43::GFP
B
tir-1(tm3036)
odr-3p::unc-43::GFP
C
n.s.
UNC-43::GFP intensity (A.U.)
in AWC axons
80
60
40
20
0
wild type
tir-1(tm3036)

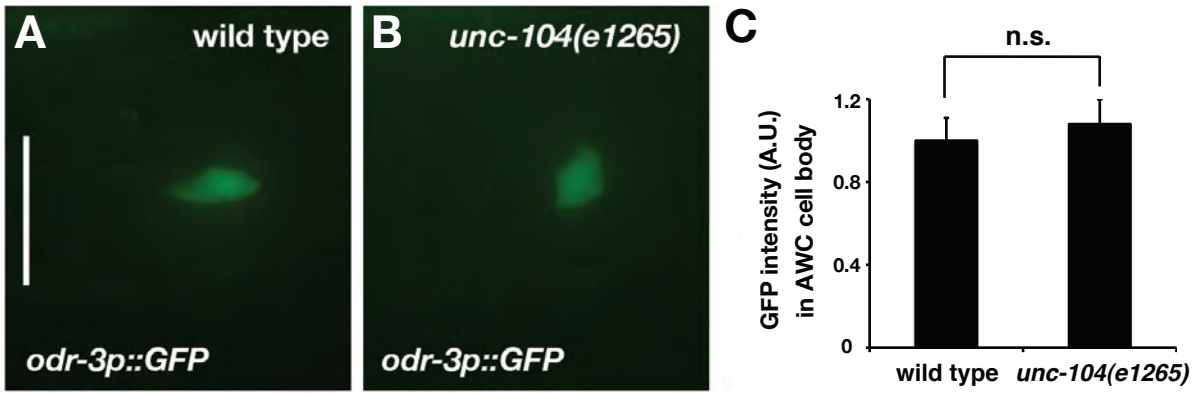
A
wild type
odr-3p::GFP
B
unc-104(e1265)
odr-3p::GFP
C
n.s.
GFP intensity (A.U.)
in AWC cell body
1.2
0.8
0.4
0
wild type
unc-104(e1265)